Thermochimica Acta, 214 (1993) 291–303
Elsevier Science Publishers B.V., Amsterdam

Kinetics and mechanism of thermal decomposition of lithium oxalate catalysed by $Cd_{1-x}Co_xFe_2O_4$ ($x = 0.0$, 0.5 and 1.0) ferrospinel additives

M.M. Girgis and A.M. El-Awad

Chemistry Department, Faculty of Science, Assiut University, Assiut (Egypt)

(Received 14 May 1992)

Abstract

The thermal decomposition of lithium oxalate ($Li_2C_2O_4$) in air was investigated by means of TG, DTA, X-ray and scanning electron microscopic (SEM) techniques. The non-isothermal study reveals that lithium oxalate decomposes in one step to the carbonate. The kinetics of the isothermal decompositon of the pure salt were studied in the temperature range 556–585°C. The fraction decomposed (α) against time (t) curves were sigmoid in shape with relatively long induction periods of the onset of salt breakdown. The kinetic parameters of the decomposition reaction were deduced employing a computer-oriented kinetic analysis of the α'–t' data. This indicates that the decomposition process is governed by the random nucleation Erofe'ev equation over the entire temperature range. The kinetic evidence was supported by SEM observations. In order to evaluate the effect of $Cd_{1-x}Co_xFe_2O_4$ ($x = 0.0$, 0.5 and 1.0) ferrospinels on the thermal decomposition reaction, the decomposition of $Li_2C_2O_4$ was followed in the presence of 10 wt.% of the additive. The results show that these ferrites promote the thermal decomposition rates of the oxalate with increasing x in the order $0.0 < 0.5 < 1.0$. In the presence of these additives also the decomposition reaction obeys the Erofe'ev equation and proceeds by the nucleation-and-growth mechanism. The promotional effect of these catalysts is described. Their activity in promoting salt breakdown is a consequence of their appreciable solubility in the host oxalate crystals.

INTRODUCTION

The metal salts or organic acids provide a group of related substances which permit comparison of the effects of variations of either the cation or the anion on their thermal stability. Extensive and intensive studies of the thermal analysis and kinetics of thermal decomposition of metal oxalates have attracted the interest of several investigators [1(a)–6]. Some of these salts have been considered as economical catalyst precursors [7]. How-

Correspondence to: M.M. Girgis, Chemistry Department, Faculty of Science, Assiut University, Assiut, Egypt.

ever, the results obtained in studying the kinetics of thermal decomposition reactions showed discrepancies between different workers [4–6], and many causes have been cited to explain the deviations in the results. Dollimore and Tinsley [8] studied the DT–TG analysis and kinetics of decomposition of lithium oxalate to the carbonate in an atmosphere of nitrogen. The reaction kinetics were reported [8] to follow a phase boundary mechanism up to 95% reaction. Lithium carbonate is used as a flux in porcelain enamel formulations, in the production of special toughened glasses and of aluminium of low cost and high production capacity, and as an effective treatment for manic-depressive psychoses [9].

It has been shown in many studies that the mechanical addition of a foreign substance to metallic salts gives rise to changes in the thermochemical reaction behaviour of the salt [1(b), 10–12]. These changes may be due to (i) the chemical reaction occurring between the reactant and additive to form stable compounds [10], and (ii) the catalytic action of additive in accelerating or decelerating the reaction [1(b), 11, 12]. The present article extends studies of the thermal decomposition of lithium oxalate in air in order to investigate the role of $Cd_{1-x}Co_xFe_2O_4$ catalysts in promoting the decomposition to the carbonate. This study demonstrates that the decompositions of oxalates are individual processes, and lithium oxalate decomposition in air exhibited no obvious close relationships with the analogous reaction in nitrogen or with the similar reactions in air of the other oxalates.

EXPERIMENTAL

Lithium oxalate was a Hopkin & Williams product (UK). All other reagents were of analytical grade (BDH Chemicals) and used without purification. Cadmium cobalt iron oxide ferrospinels ($Cd_{1-x}Co_xFe_2O_4$, where $x = 0.0$, 0.5 or 1.0) were synthesized by using the corresponding metal nitrate as described elsewhere [13]. The mixing of lithium oxalate with 10 wt.% of spinel additives, as thermally stable solid catalysts, was carried out in an agate mortar. Twenty minutes were needed to obtain a homogeneous mixture. In experiments without additives, the pure sample was also ground for 20 min. The non-isothermal decomposition of the pure salt and of the salt mixed with catalysts was studied using thermogravimetric analysis (TGA) to monitor the percentage decomposed versus temperature [14]. Differential thermal analysis (DTA) experiments were performed on an automatically recording Shimadzu apparatus, type DT 40 H, in air. α-Al_2O_3 was used as the reference solid and the rate of heating was standardized at 10°C min^{-1}. The study of isothermal kinetics [15] of pure and mixed samples was carried out with the aid of a Sartorius electrobalance (Type 2004 MP6). The sample (500 mg) was placed in a quartz basket suspended from the arm of the balance by means of a quartz

wire. The sample temperature was adjusted using a Heraeus temperature controller Type TRK. The temperature variation during any run was better than ±0.5°C. A Philips X-ray diffractometer (model PW 1710) was used to record *d* values for the residual material at different temperatures and at various stages of decomposition. Scanning electron microscopic (SEM) examinations were performed on a JEOL JSM-T 200 scanning microscope (JEOL, Tokyo, Japan). The samples were prepared by sprinkling the powder lightly onto a double-sided adhesive tape, which was mounted on a SEM specimen stub. The edge of the double-sided tape was coated with silver paint to minimize charging. Finally, the sample was sputter coated with gold. Micrographs were obtained in secondary electron imaging mode using a potential difference of 25 kV. SEM observations were carried out at a magnification of ×500–1500. SEM examinations were made of the reactant after decomposition to various known fractional extents of reaction (α) and after completion of the reaction.

RESULTS AND DISCUSSION

Figure 1 shows the thermogravimetric analysis curves for pure and mixed lithium oxalate samples obtained in air as described elsewhere [14]. The corresponding differential thermal analysis curves are represented in Fig. 2. Pure lithium oxalate decomposes in one step to the carbonate, so that it does not occur in a hydrated form, as reported previously [8]. The

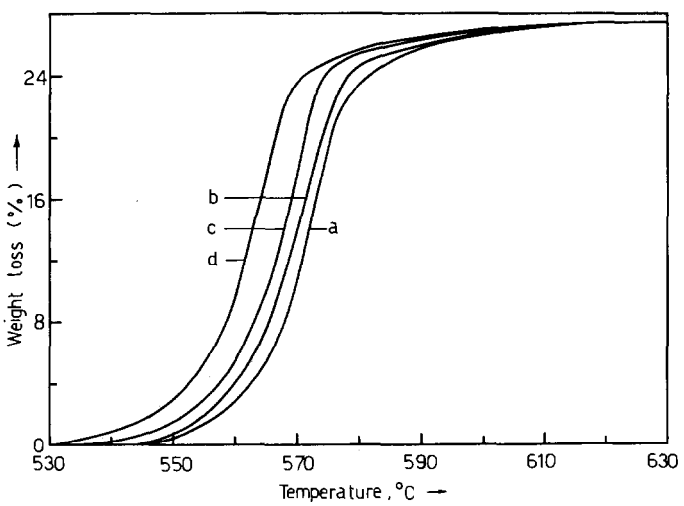

Fig. 1. Thermogravimetric curves for the non-isothermal decomposition of pure lithium oxalate and its mixture with 10 wt.% $CdFe_2O_4$, $Cd_{0.5}Co_{0.5}Fe_2O_4$ and $CoFe_2O_4$ (curves a–d respectively).

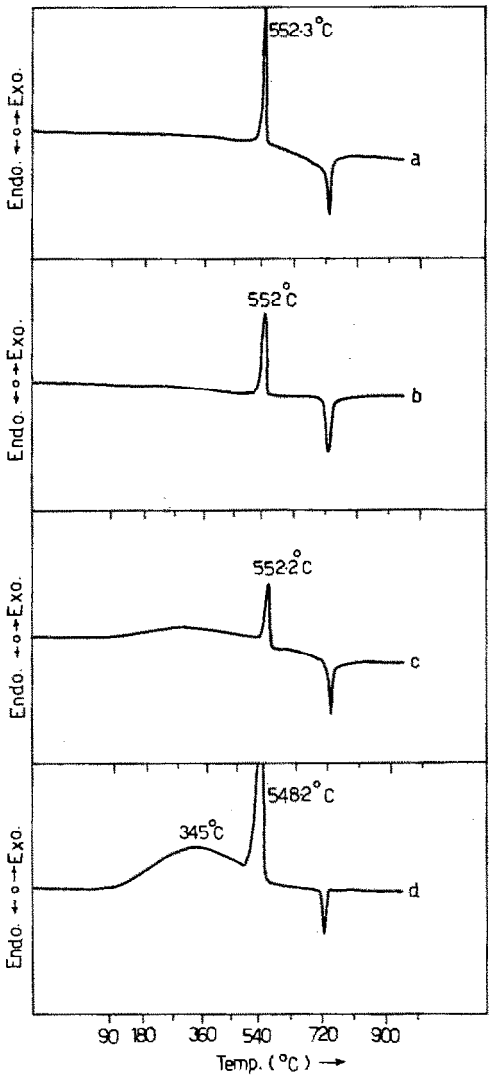

Fig. 2. DTA curves for the decomposition of pure lithium oxalate and its mixtures with the additives (symbols as in Fig. 1).

weight loss recorded for this stage was 27.4%, which matched with the calculated theoretical value. The DTA curve for the pure salt showed an exothermic decomposition to the carbonate at 552.3°C. In this context, the X-ray diffraction pattern for the pure sample calcined at 569°C showed the diffraction lines of Li_2CO_3 [16] with *d* spacings of 2.81, 4.17, 2.93, 2.43, 2.63, 3.03, 3.80, and 2.49; Fig. 3.

The kinetics of the isothermal measurements were examined to extend the systematic investigation of the decomposition of pure $Li_2C_2O_4$ to Li_2CO_3 in the range 556–585°C. The results obtained from the constant-

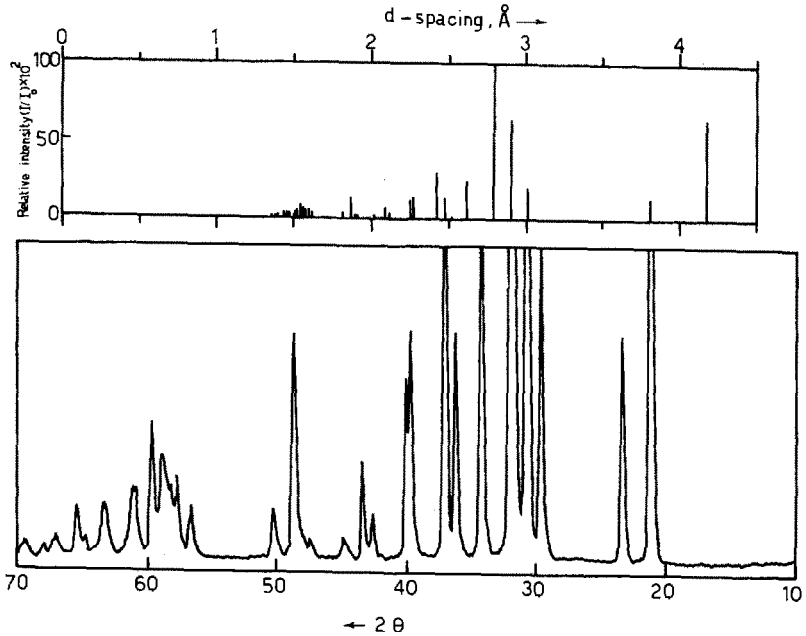

Fig. 3. XRD pattern for the calcination product, at 569°C, of pure lithium oxalate.

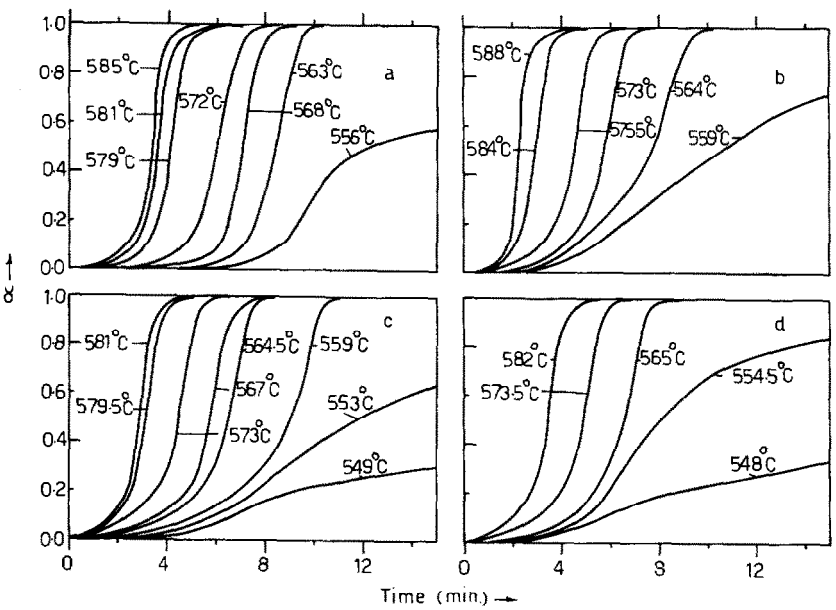

Fig. 4. Representative α vs. time curves for the isothermal decomposition of pure lithium oxalate and its mixtures with the additives (symbols as in Fig. 1).

temperature experiments were plotted as fraction decomposed (α) against time (t) for each temperature; Fig. 4(a). The curves were characteristically sigmoid in shape with an induction period [17] (t_0) to the onset of salt breakdown. This period includes the initial slow processes which subsequently culminate in the establishment of the growth interface that is the active participant in the main decomposition process. The induction period which was relatively long, depended on the decomposition temperature (Fig. 3). After completion of an initial rate process at α_i, the main reactions were analysed according to the kinetic models [18] listed in Table 1, where α and t were modified [1(c), 17] to α' and t', respectively, by subtraction of the contribution of the initial process, where $\alpha' = (\alpha - \alpha_i)/(1 - \alpha_i)$ and $t' = (t - t_0)$. Under isothermal conditions, the rate constant k is independent of reaction time, and so $kt' = g(\alpha')$. A plot of $g(\alpha')$ vs. time (t') should thus give a straight line if the correct form of $g(\alpha')$ is used. The function $g(\alpha')$ depends on the mechanism controlling the reaction and on the size and shape of the reacting particles [19].

The computer-oriented kinetic analysis was performed for each set of

TABLE 1

Kinetic equations $[g(\alpha') = k(t')^a]$ examined in this work

$g(\alpha')^b$	Function symbol	Rate-controlling process
$(\alpha')^2$	D_1	One-dimensional diffusion
$\alpha' + (1 - \alpha')\ln(1 - \alpha')$	D_2	Two-dimensional diffusion
$[1 - (1 - \alpha')^{1/3}]^2$	D_3	Three-dimensional diffusion (Jander equation)
$(1 - \frac{2}{3}\alpha') - (1 - \alpha')^{2/3}$	D_4	Three-dimensional diffusion (Ginstling–Brounshtein equation)
$[1 - (1 - \alpha')^{1/2}]$	R_2	Two-dimensional phase boundary reaction
$[1 - (1 - \alpha')^{1/3}]$	R_3	Three-dimensional phase boundary reaction
$-\ln(1 - \alpha')$	F_1	First-order kinetics
$[-\ln(1 - \alpha')]^{1/2}$	A_2	Random nucleation (Avrami equation)
$[-\ln(1 - \alpha')]^{1/3}$	A_3	Random nucleation (Erofe'ev equation)
$\ln[\alpha'/(1 - \alpha')]$		Random nucleation (Prout–Tompkins equation)

[a] Times were corrected for any induction period (t_0), $t' = (t - t_0)$.

[b] The contributions of the initial process (α_i) were subtracted; $\alpha' = (\alpha - \alpha_i)/(1 - \alpha_i)$, where $\alpha_i = 0.04$.

the isothermal α'/t' data using the different kinetic equations. The results indicated that the random nucleation Erofe'ev [20] equation (A_3 function) gives the best fit of the data, with a correlation coefficient very close to unity. The time required for the precursors to nucleus generation to be transformed into fully active growth nuclei is the induction period observed in Fig. 1(a). Here, the nucleation process involves conversion of a small volume of reactant into a stable particle of product, and continued reaction (growth) occurs preferentially at the interfacial zone of contact between these two phases [1(d)]. As nuclei grow larger they must eventually impinge on one another, so that growth ceases where they

TABLE 2

Kinetic parameters obtained by a computer analysis of the isothermal decomposition of pure lithium oxalate and its mixtures with 10 wt% $CdFe_2O_4$, $Cd_{0.5}Co_{0.5}Fe_2O_4$ and $CoFe_2O_4$ additives

No.	Substance	Temp. (°C)	Parameter		
			10^4k (s^{-1})	E_a (kJ mol^{-1})	ln A (s^{-1})
1	Pure lithium oxalate	556	6.53	269.2	31.8
		563	8.93		
		568	11.39		
		572	13.73		
		579	18.95		
		581	21.08		
		585	24.73		
2	Lithium oxalate +$CdFe_2O_4$	559	8.80	263.7	27.3
		564	10.86		
		573	16.54		
		575.5	18.38		
		584	26.68		
		588	31.38		
3	Lithium oxalate +$Cd_{0.5}Co_{0.5}Fe_2O_4$	549	6.93	244.7	28.6
		553	8.21		
		559	10.74		
		564.5	13.54		
		567	15.10		
		573	19.38		
		579.5	25.05		
		581	27.27		
4	Lithium oxalate +$CoFe_2O_4$	548	6.98	212.6	23.9
		554.5	8.89		
		565	13.15		
		573.5	17.82		
		582	24.01		

touch. Accordingly, we can conclude that initial nucleation occurs on the surface followed by growth of the product from the surface towards the interior. Table 2 gives the kinetic parameters for the decomposition of $Li_2C_2O_4$ to Li_2CO_3 in air.

Application of the Arrhenius equation using the data depicted in Table 2

$$k = A \exp(-E_a/RT) \quad (1)$$

where E_a is the energy of activation and A is the pre-exponential factor, provides the two values $E_a = 269.2\ \text{kJ mol}^{-1}$ and $\ln A = 31.8\ \text{s}^{-1}$ for the thermal decomposition of lithium oxalate (Figure 5, curve a).

Kinetic evidence alone cannot provide positive proof of the operation of a particular mechanism [21]. The sizes of the reactant crystallites made it possible to characterize by microscopy [22, 23] the systematic changes in the textural features of the surface as well as in the reaction geometry that occurred during the progress of the decomposition. Therefore, scanning electron-microscopic examinations were carried out at known fractional reaction values $\alpha = 0.0$, 0.3, 0.8 and 1.0.

The appearance and significant textural characteristics of typical lithium oxalate crystallites ($\alpha = 0.0$) are shown in Fig. 6 (plates a_1 and a_2). It is

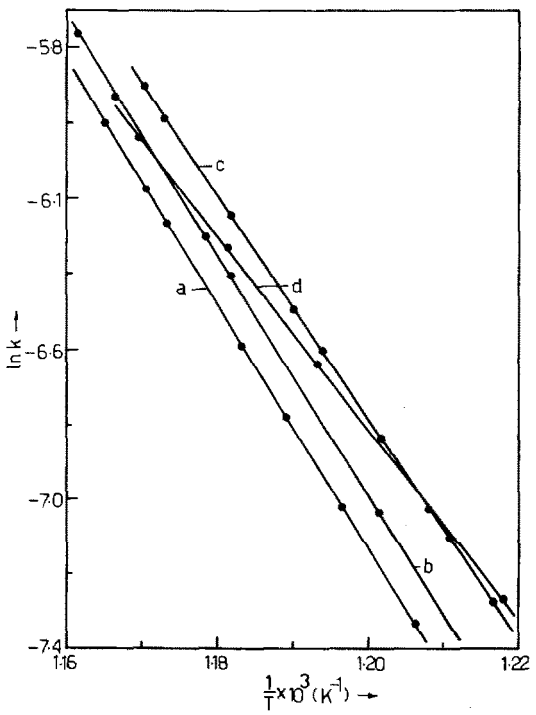

Fig. 5. Arrhenius plots for the isothermal decomposition of prue lithium oxalate and its mixtures with the additives (symbols as in Fig. 1).

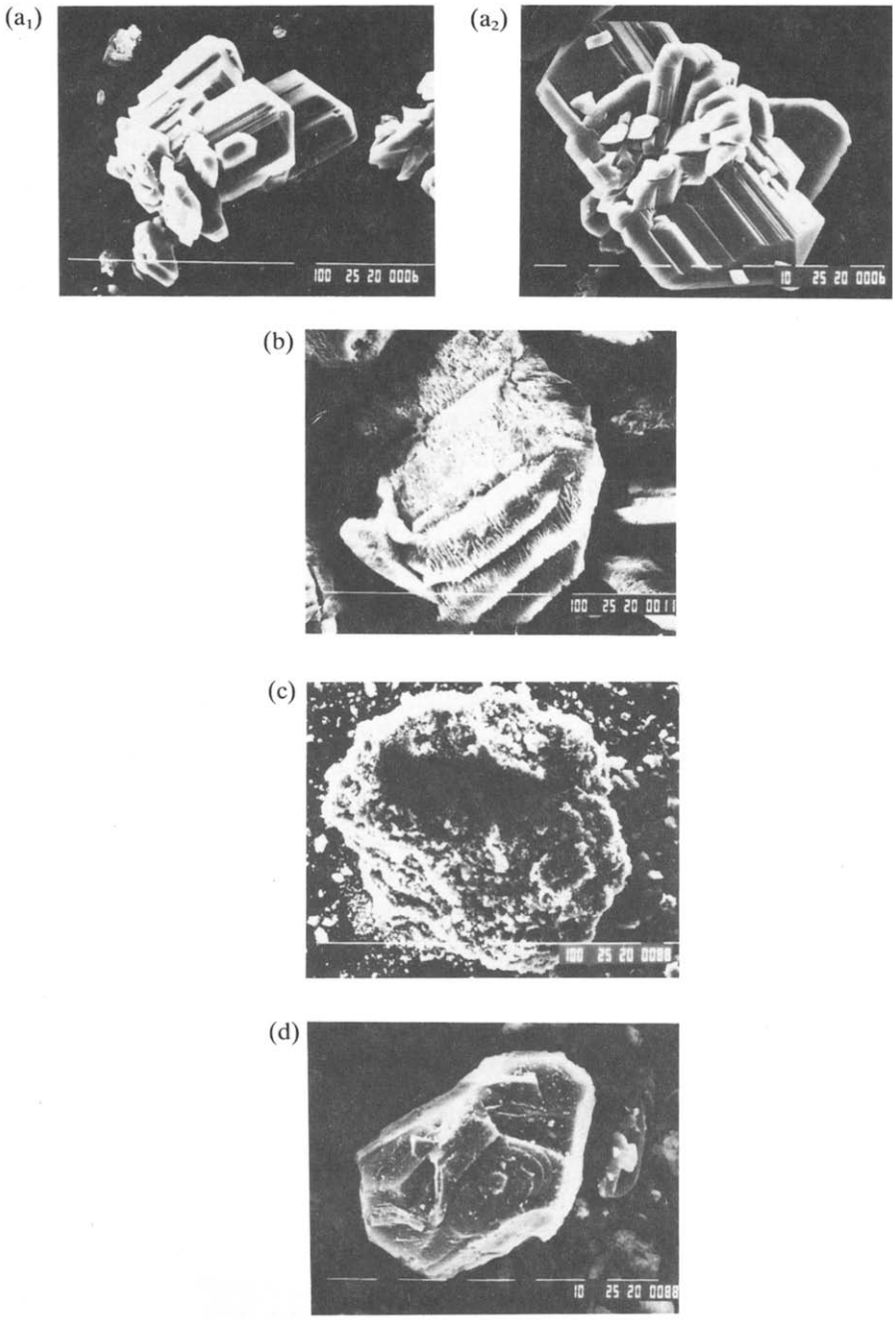

Fig. 6. Key: (a_1 and a_2) scanning electron micrographs showing typical crystals of undecomposed ($\alpha = 0.0$) lithium oxalate (a_1, original magnification ×750; a_2, original magnification ×1000); (b) lithium oxalate crystallites decomposed in air to $\alpha = 0.3$ at 569°C (b, original magnification ×750); (c) lithium oxalate crystallites decomposed in air to $\alpha = 0.8$ at 569°C (c, original magnification ×500); (d) completely decomposed ($\alpha = 1.0$) crystallites of lithium oxalate (d, original magnification ×1500).

clear that surfaces were approximately planar, some included pits, and crystallite corners were sharp. A characteristic feature of surface texture was parallel surface striations, "terracing", of the approximately planar boundaries. Aggregates of many small crystallites were also present.

Figure 6, plate b is a replica of slightly damaged ($\alpha = 0.3$) reactant crystallites. It indicates that, during the early stages of decomposition, numerous pits and pores appeared on the surface. There is no indication of melting or cracking of the reactant particles. The perceptible change is the textural modification of the crystal surfaces. there was some surface roughening during reaction and a local development of crystal surface areas [8] having textural features of the solid product, which adheres to the surface in the partly decomposed salt. This can be identified as a nucleus composed of a coherent, asymmetric region of product extending on the surface. Such growth of compact product assemblages without melting can therefore be regarded as an example of functional nuclei [24], wherein Li_2CO_3 actively catalyses salt breakdown.

The SEM photograph for the $\alpha = 0.8$ sample (Fig. 6, plate c) reflects the systematic morphological changes during the growth process, and indicates that the overlapping of the product nuclei takes place through their growth process, where irregularly shaped fragments of product covered most of the surface of the product assemblages.

On completion of reaction ($\alpha = 1.0$), a drastic change in texture and crystallinity were observed; see Fig. 6 (plate d). This is also confirmed by X-ray diffraction measurements for complete salt decomposition, where intense lines were obtained (Fig. 3(b)). Dollimore and Tinsley [8] noticed a marked increase in surface area during the initial stages of decomposition was later followed by extensive sintering, which is in agreement with our microscopic observations.

Thus, the microscopic evidence and the pattern of kinetic obedience to the Erofe'ev equation together provide direct confirmation that the decomposition reaction of $Li_2C_2O_4$ in air proceeds by a solid-state random nucleation followed by a growth process in the acceleratory region. Our results are in agreement with previous kinetic studies on some other oxalates [1, 19, 25–29]. An agreement between the results of the present kinetic analysis in air and the previous investigation in a nitrogen atmosphere is not expected, on account of the difference in the sample and measuring conditions such as pretreatment, crystallite sizes, shapes, imperfections, size distributions, texture, packing, atmosphere, temperature and other parameters which can influence the decomposition rates and mechanism of different salt preparations or pre-treated samples [30, 31].

Studies of the influence of additives on salt decomposition processes are often directed towards the determination or confirmation of the decomposition mechanism of the pure compound [32]. These investigations are frequently qualitative, and kinetic conclusions may not extend beyond the

comment that a particular additive accelerates, inhibits or is without influence on the decomposition process. Therefore, the thermal decomposition of lithium oxalate was investigated non-isothermally and isothermally in the presence of three catalysts of general formula $Cd_{1-x}Co_xFe_2O_4$, with $x = 0.0$, 0.5 and 1.0. These additives were characterized structurally and were pre-tested in other catalytic reactions [13, 21, 33, 34]. Examination of the corresponding TG curves for lithium oxalate mixed with $CdFe_2O_4$, $Cd_{0.5}Co_{0.5}Fe_2O_4$ and $CoFe_2O_4$ (Fig. 1, curves b, c and d, respectively) shows that all these additives accelerate to different extents the thermal decomposition of the salt, there is some diminution of the induction period, and 10 wt% of $CoFe_2O_4$ has a remarkable promotional effect.

In order to relate the promotional behaviour of the additives to a parameter indicative of their catalytic activity, the patterns of the kinetic (α, t) data exhibited by the different additives constituting the present study were analysed, and are summarized in Fig. 4, curves b, c and d. The analysis of the kinetic data was performed in a way similar to that adopted for the pure sample. The results indicate that the decomposition process obeys the Erofe'ev equation [20], where the nucleation-and-growth mechanism can be put forward to describe the course of decomposition of lithium oxalate in the presence of catalyst additives. The activation energy values, as indicative kinetic parameters, were also obtained using the Arrhenius equation (Fig. 5, curves b–d). The results are given in Table 2. The observed reduction in activation energy values, in ascending order $x = 0.0$, 0.5 and then 1.0, represents a parallelism to the promotional effect of these additives, where $x = 1.0$ has the maximum activity; see Fig. 1.

The DTA curves for lithium oxalate mixed with $CdFe_2O_4$, $Cd_{0.5}Co_{0.5}Fe_2O_4$ and $CoFe_2O_4$ are represented in Fig. 2, curves b, c and d, respectively. A comparative study of these curves reveals that the ferrospinel additives have little effect on the exothermic decomposition of lithium oxalate to the carbonate. It has been reported [1(a), 35] that the thermal decomposition of oxalates to carbonates proceeds according to eqns. (2)–(4), where the initial breakdown step was identified as C–C bond rupture in the $C_2O_4^{2-}$ anion.

$$C_2O_4^{2-} \rightleftharpoons 2CO_2^- \tag{2}$$

$$2CO_2^- \rightarrow [OCOCO_2]^{2-} \tag{3}$$

$$[OCOCO_2]^{2-} \rightarrow CO_3^{2-} + CO \tag{4}$$

This intermediate may be converted to the carbonate through the carbonylcarbonate intermediate. The activation energy found for the decomposition of an individual oxalate ion in a KBr matrix (270 ± 15 kJ mol^{-1}) [36, 37] is regarded as the energy required for C–C bond

rupture. This means that the decomposition temperature may be governed by the bond's dissociation energy. If the rate determining step is the C–C bond rupture in the oxalate, it is reasonable that the semiconductive ferrospinel additives show no effect, since the rupture does not accompany the electron transfer.

The additive effects on the non-isothermal and isothermal decomposition processes can be understood on the basis of the suggestion of Boldyrev [38] that the additives may cause lattice defects or deformation of the lattice, which in turn will affect the thermal decomposition process. The three ferrite additives accelerate to different extents the thermal decomposition of the oxalate, and $CoFe_2O_4$ has the most pronounced promotional effect; see Fig. 1. The disappearance of d spacing values characterizing the ferrite structure in the lithium oxalate–ferrospinel mixtures on raising the reaction temperature was observed experimentally. This confirms the appreciable solubility of these additives in the host matrix [21]. Decomposition to the carbonate proceeded more easily in the presence of cobalt ions because of the lowest standard heat of formation ($-\Delta H_f^{\ominus}$) of their carbonate salt compared with those of cadmium of lithium ions [39(a)]. This suggestion was supported by the DTA results, where a wide exothermic effect covering the temperature range 316–383°C was observed in the presence of $CoFe_2O_4$ additives, which can be correlated with the formation of $CoCo_3$ salt [1(e)].

Finally, the pronounced promotional effect observed for $CoFe_2O_4$ additives can be ascribed to (i) their high lattice oxygen (O^{2-}) content [33, 34] and (ii) the higher redox potential of the electronic reaction ($Co^{2+} + 2e^- \rightarrow Co$) relative to those of the other two (Cd and Fe) ions [39(b)]. These parameters force us to suggest the following additional steps:

$$O^{2-} \rightarrow 0.5O_2 + 2e^- \quad (5)$$

$$CO + 0.5O_2 \rightarrow CO_2 \quad (6)$$

$$Co^{2+} + 2e^- \rightarrow Co \quad (7)$$

which take place parallel to the previously described three steps of eqns. (2)–(4). Accordingly, the formation of Co atoms represents new embryos which induce more nucleated centres to promote the oxalate breakdown.

REFERENCES

1 M.E. Brown, D. Dollimore and A.K. Galwey, in C.H. Bamford and C.F.H. Tipper, Reactions in the Solid State, Comprehensive Chemical Kinetics, Vol. 22, Elsevier, Amsterdam, 1980: (a) p. 218; (b) p. 260; (c) p. 80; (d) p. 42; (e) p. 221.
2 C.G.R. Nair and K.N. Ninan, Thermochim. Acta, 23 (1978) 161; 30 (1979) 25.
3 H. Tanaka, S. Ohshima, S. Ichiba and N. Negita, Thermochim. Acta, 48 (1981) 137; H. Tanaka, S. Ohshima and N. Negita, Thermochim. Acta, 53 (1982) 387.
4 P.O. Brien and S.D. Ross, Thermochim. Acta, 53 (1982) 195.

5 A.M. Gadalla, Thermochim. Acta, 74 (1984) 255.
6 A.R. Salvador, E.C. Calvo and J.M. Navarro, Thermochim. Acta, 87 (1985) 163.
7 V.V. Boldyrev, M. Bulens and B. Deman, The Control of the Reactivity of Solids, Elsevier, Amsterdam, 1979.
8 D. Dollimore and D. Tinsley, J. Chem. Soc. A, 19 (1971) 3043.
9 N.N. Greenwood and A. Earnshaw, Chemistry of the Elements, Pergamon Press, Oxford, 1984, p. 77.
10 T. Ishii, R. Furuichi and Y. Kobayashi, Thermochim. Acta, 9 (1974) 39.
11 R. Furuichi, T. Ishii and K. Kobayashi, J. Therm. Anal., 6 (1974) 305.
12 M. Shimokawabe, R. Furuichi and T. Ishii, Thermochim. Acta, 20 (1977) 347; 21 (1977) 237; 24 (1978) 69.
13 R.M. Gabr, M.M. Girgis and A.M. El-Awad, Langmuir, 7 (1991) 1642.
14 R.M. Gabr, M.M. Girgis and A.M. El-Awad, Thermochim. Acta, 196 (1992) 279.
15 R.M. Gabr, A.M. El-Awad and M.M. Girgis, J. Therm. Anal., 37 (1991) 249.
16 W.F. McClune (Ed.), JCPDS Powder Diffraction File (Inorganic Phases), Search Manual (Hanawalt), JCPDS, 1983.
17 A.K. Galwey, P.J. Herley and M.A. Mohamed, J. Chem. Soc. Faraday Trans. 1, 84 (1988) 729.
18 K.N. Ninan and C.G.R. Nair, Thermochim. Acta, 30 (1979) 25.
19 S.N. Basahel, A.Y. Obaid and E.M. Diefallah, Radiat. Phys. Chem., 29 (1987) 447.
20 A.K. Galwey and M.A. Mohamed, J. Chem. Soc. Faraday Trans. 1, 81 (1985) 2503.
21 R.M. Gabr, A.M. El-Awad and M.M. Girgis, Thermochim. Acta, 194 (1992) 47.
22 L.G. Harrison, C.H. Bamford and C.F.H. Tipper, Comprehensive Chemical Kinetics, Vol. 2, Elsevier, Amsterdam, 1969, Chap. 5.
23 A.K. Galwey, D.M. Jamieson, M.E. Brown and M.J. McGinn, Reaction Kinetics in Heterogeneous Chemical Systems, Elsevier, Amsterdam, 1975, p. 520.
24 A.K. Galwey, Proc. 7th Int. Conf. Thermal Analysis, Kingston, Ont., Wiley, New York, 1982, p. 38.
25 A. Finch, P.W.M. Jacobs and F.C. Tompkins, J. Chem. Soc., (1954) 2053.
26 A.G. Leiga, J. Phys. Chem., 70 (1966) 3254; 3260.
27 P.W.M. Jacobs and A.R.T. Kureishy, Trans. Faraday Soc., 58 (1962) 551.
28 L. Tournayan, H. Charcosset, H.R. Wheeler, J.M. McGinn and A.K. Galway, J. Chem. Soc. A, (1971) 686.
29 T. Palanismy, T. Gopalakrishnan, B. Vismanathan, V. Srinivasan and M.V.C. Sastri, Thermochim. Acta, 2 (1971) 265.
30 G.D. Anthony and P.D. Garn, J. Am. Ceram. Soc., 57 (1974) 132.
31 P.W.M. Jacobs and F.C. Tompkins, in W.E. Garner (Ed.), Chemistry of the Solid State, Butterworth, London, 1955, p. 187.
32 A.M. El-Awad, R.M. Gabr and M.M. Girgis, Thermochim. Acta, 184 (1991) 205.
33 R.M. Gabr, M.M. Girgis and A.M. El-Awad, J. Mater. Chem. Phys., 28 (1991) 413.
34 M.M. Girgis and A.M. El-Awad, Material Chemistry and Physics, in press.
35 V.V. Boldyrev, I.S. Nev'yantsev, Yu. I. Mikhailov and E.F. Khairetdinov, Kinet. Katal., 11 (1970) 367.
36 K.O. Hartman and I.C. Hisatsune, J. Phys. Chem., 69 (1965) 583; 70 (1966) 1281; 71 (1967) 392.
37 F.E. Freeberg, K.O. Hartman, I.C. Hisatsune and J.M. Schempf, J. Phys. Chem., 71 (1967) 397.
38. V.V. Boldyrev, Kinet. Katal., 1 (1960) 203.
39 R.C. Weast and M.J. Astle, CRC Handbook of Chemistry and Physics, CRC Press, Boca Raton, FL, 61st Edn., 1980–1981: (a) p. D-67; (b) p. D-155.